

Article

Open Access



# Sustainable off-grid gasification: co-production of electricity, heat, and activated carbon

Jakub Čespiva<sup>1,\*</sup> , Agata Mlonka-Mędrala<sup>2,\*</sup> , Małgorzata Sieradzka<sup>3</sup> , Wojciech Kalawa<sup>2</sup> , Marcin Sowa<sup>2</sup> , Lukasz Niedzwiecki<sup>4,5</sup> , Jan Skřínský<sup>1</sup> , Marek Jadlovec<sup>6</sup> , Jan Výtisk<sup>6</sup> , Sangeetha Thangavel<sup>7,8</sup> , Xuebin Wang<sup>9</sup> , Wei-Hsin Chen<sup>10,11,12</sup>

<sup>1</sup>Energy Research Centre, Centre for Energy and Environmental Technologies, VSB - Technical University of Ostrava, Ostrava 70800, Czech Republic.

<sup>2</sup>Department of Thermal and Fluid Flow Machines, Faculty of Energy and Fuels, AGH University of Science and Technology, Kraków 30-059, Poland.

<sup>3</sup>Faculty of Metals Engineering and Industrial Computer Science, AGH University of Science and Technology, Kraków 30-059, Poland.

<sup>4</sup>Department of Civil, Environmental and Mechanical Engineering, University of Trento, Trento 38123, Italy.

<sup>5</sup>Faculty of Mechanical and Power Engineering, Department of Energy Conversion Engineering, Wrocław University of Science and Technology, Wrocław 50-370, Poland.

<sup>6</sup>Faculty of Mechanical Engineering, Department of Energy, VSB - Technical University of Ostrava, Ostrava 70800, Czech Republic.

<sup>7</sup>Department of Energy and Refrigerating Air-Conditioning Engineering, National Taipei University of Technology, Taipei 10608, Taiwan.

<sup>8</sup>Research Center of Energy Conservation for New Generation of Residential, Commercial, and Industrial Sectors, National Taipei University of Technology, Taipei 10608, Taiwan.

<sup>9</sup>MOE Key Laboratory of Thermo-Fluid Science and Engineering, Xi'an Jiaotong University, Xi'an 710049, China.

<sup>10</sup>Department of Aeronautics and Astronautics, National Cheng Kung University, Tainan City 701401, Taiwan.

<sup>11</sup>Research Center for Smart Sustainable Circular Economy, Tunghai University, Taichung City 407224, Taiwan.

<sup>12</sup>Department of Mechanical Engineering, National Chin-Yi University of Technology, Taichung City 411030, Taiwan.

**\*Correspondence to:** Dr. Jakub Čespiva, Energy Research Centre, Centre for Energy and Environmental Technologies, VSB - Technical University of Ostrava, 17. Listopadu (Non-Capitalised L) 2172/15, Ostrava 70800, Czech Republic. E-mail: jakub.cespiva@vsb.cz; Prof. Agata Mlonka-Mędrala, Department of Thermal and Fluid Flow Machines, Faculty of Energy and Fuels, AGH University of Science and Technology, Al. Mickiewicza 30, Kraków 30-059, Poland. E-mail: amlonka@agh.edu.pl

**How to cite this article:** Čespiva, J.; Mlonka-Mędrala, A.; Sieradzka, M.; Kalawa, W.; Sowa, M.; Niedzwiecki, Ł.; Skřínský, J.; Jadlovec, M.; Výtisk, J.; Thangavel, S.; Wang, X.; Chen, W. H. Sustainable off-grid gasification: co-production of electricity, heat, and activated carbon. *Energy Mater.* 2025, 5, 500017. <https://dx.doi.org/10.20517/energymater.2024.104>

**Received:** 2 Aug 2024 **First Decision:** 12 Sep 2024 **Revised:** 4 Oct 2024 **Accepted:** 17 Oct 2024 **Published:** 10 Jan 2025

**Academic Editors:** Sining Yun, Hu Li **Copy Editor:** Fangling Lan **Production Editor:** Fangling Lan

## Abstract

The process of gasification is well-known; however, to this day, the applications of such facilities, especially off-grid small-scale units for direct electricity and char production, are scarce. In this study, an off-grid fixed bed downdraft



© The Author(s) 2025. **Open Access** This article is licensed under a Creative Commons Attribution 4.0 International License (<https://creativecommons.org/licenses/by/4.0/>), which permits unrestricted use, sharing, adaptation, distribution and reproduction in any medium or format, for any purpose, even commercially, as long as you give appropriate credit to the original author(s) and the source, provide a link to the Creative Commons license, and indicate if changes were made.



gasification unit is studied from the gaseous/solid product character perspective. This unit represents a possible solution for the emerging call for sustainable decentralised energy sources. Softwood chips were utilised in this study, and their conversion into synthetic gas (direct electricity supply) and solid biochar was observed and analysed. The results show promising values of synthetic gas for potential utilisation in different applications outside the direct combustion process, such as microbial syngas fermentation, with a lower heating value equal to  $6.31 \text{ MJ}\cdot\text{m}^{-3}$ . It appears that during the steam activation process of biochar, both high-quality off-gas of more than 70%<sub>vol.</sub>  $\text{H}_2$  (excluding  $\text{N}_2$ ) and activated carbon of a specific surface area of  $565.87 \text{ m}^2\cdot\text{g}^{-1}$  can be collected. Further investigations have revealed specific degradation of chemical bonds and material morphology changes during steam gasification. The microporous structure and high specific surface area of the material make it an attractive material for further development as an adsorbent in sorption cooling devices. Therefore, the waste generated within the gasification process is minimised, and the potential of the obtained products will be valued in favour of the sustainability of the remote locations.

**Keywords:** Waste management, sustainability, gasification, biochar, circular economy, off-grid

## INTRODUCTION

The gasification process is gaining attention, especially with the rising energy and environmental crises worldwide. The desire to replace expensive energy sources with available waste materials is significant and is not limited to developing countries<sup>[1]</sup>. Such an aspiration can be sustained with the application of small-scale gasification units capable of producing direct electrical energy and heat for local uses and needs while utilising local energy sources, such as wood, crop or production residues based on biomass or other hydrocarbon substances. Such materials are usually easy to combust<sup>[2,3]</sup>; however, heat energy is often optional by the operator, and the production of electricity from heat is challenging and expensive as an investment.

On the other hand, small-scale gasification equipped with simple gas cleaning technology and a piston combustion engine attached to an electrical generator can represent a cheap and moderate approach to sustainable energy management at the regional level<sup>[4]</sup>. Such an energy system can stand alone and be perfectly off-grid and independent<sup>[5,6]</sup>. Several studies reported on the performance of small-scale domestic combined heat and power (CHP) using downdraft gasifiers, including hemp farm application<sup>[4]</sup>, municipal green waste gasification<sup>[7]</sup> or river driftwood utilisation<sup>[8]</sup>. Especially in connection to rural areas or newly developed post-coal mining areas<sup>[9]</sup>, this approach appears to be particularly beneficial because, apart from the combusted gas and generated electricity, an interesting by-product material - biochar, can be generated and utilised.

Such biochar can be derived basically from any biomass-based material, such as wood pellets<sup>[10]</sup>, torrefied wood chips<sup>[11]</sup> or pistachio shells<sup>[12]</sup>. Non-biomass-based materials, such as waste tyres<sup>[13]</sup>, poultry manure<sup>[14]</sup>, and solid recovered fuel<sup>[10]</sup>, can also undergo the gasification process in the properly set conditions of the reactor. After passing through a high-temperature oxidising atmosphere, biochar loses nearly all of its water and volatile matter content; thus, it is formed mainly by carbon, oxygen and residual ash. Such material can be utilisable in numerous applications, such as the sorption of pollutants from water<sup>[15]</sup> or air/flue gas<sup>[10,16]</sup>, utilisation in adsorption chillers<sup>[17]</sup>, accumulation of the energy in carbon-based biomaterials for consequent combustion and replacement of the fossil resources or, dependent on the initial material's quality, as a nutrition-rich bearer for agricultural soil amendment<sup>[18,19]</sup>.

In the past, Phuphuakrat *et al.* produced biochar out of wood chips similar to those used in this study<sup>[20]</sup>. This biochar presented good sorption properties in the gasification tar capture issue. The same approach was examined by Shen<sup>[21]</sup>, who successfully absorbed organic pollutants and heavy metals.

The price of activated carbons used in various industries depends on the raw material from which it was obtained and on the activation method to increase its desired properties<sup>[22]</sup>. The utilisation of biomass as raw materials for activation has gained attention first due to effective waste management and second due to the low price of the feedstock. The challenge is to define the most suitable way for the pre-treatment and activation to achieve properties of waste-derived activated sorbents comparable to sorbents available on the market. According to the circular economy concept, the implementation of new products with added value is preferred over energy recovery. Steam activation is one of the most frequently used techniques in the commercial production of activated carbon from clean fuels such as wood and charcoal. Steam gasification enables an increase in the internal active surface area of the material and additionally produces valuable syngas, an energy carrier. Its other major advantage is its minor impact on the environment and small energy consumption compared to chemical activation.

Only a limited number of studies have investigated polygeneration installations that produce combustible gas suitable for engine-based CHP units and activated carbon. Tchoffor *et al.* investigated the production of syngas and activated carbon in a dual-bed fluidised gasifier<sup>[23]</sup>. However, the investigation was focused on activated carbon production, achieving surface areas ranging between 693 and 1,416 m<sup>2</sup>·g<sup>-1</sup><sup>[23]</sup>, whereas the quality of the gas was not assessed. Gañán *et al.* examined both gaseous products and activated carbon<sup>[24]</sup>. However, the experimental investigation was performed only on a laboratory scale, and no subsequent activation was performed, although the char from gasification was considered activated, resulting in surface areas between 240 and 490 m<sup>2</sup>·g<sup>-1</sup><sup>[24]</sup>.

In the presented study, a specific gasification unit, Power Pallet 30 (PP 30), is closely looked at from the energy and material production point of view. The detailed characterisation of the unit performance with softwood chips is defined, and the composition of the gaseous products (producer gas) and solid products (activated carbon) is analysed, including the composition of the off-gas from physical activation. Mapping of the inorganics on the surface of the activated carbon is investigated thoroughly.

The novelty of this study is in its comprehensive approach. Studies published so far typically focus on a single product, be it producer gas/syngas, biochar, or activated carbon. This study analyses all the products of such installation, thus providing conclusive proof that small-scale biorefinery, based on biomass gasification, is indeed capable of producing good quality gas and biochar. The gas can be used for energy generation and for the production of chemicals (e.g., by fermentation processes), whereas the biochar is suitable for subsequent activation, producing a market-ready product.

## EXPERIMENTAL

### Gasification unit

The technology utilised for the purpose of this research is based on a small-scale, commercial fixed-bed gasification reactor PP 30 (All Power Labs, USA) equipped with a heat exchanging system for efficient heat distribution along the technology<sup>[4]</sup>. This reactor was originally designed to fulfil the purpose of generating electric energy directly from biomass feedstock, especially wood chips and shells of various nuts, in places where these commodities are readily available. The grain size should range from 10 to 40 mm, and its moisture content should be below 30%<sub>wt.</sub><sup>[7]</sup>.

An automatic screw conveyor delivers the fuel from the hopper to the grate area. The residue material falls down to the drop zone and is stored in a gastight vessel. The producer gas is led through a heated duct to a cyclone barrier for a large-fraction particulate matter separation, while the fines are entrapped on a filtration cake of reversed baghouse filter candles. The tube-in-shell exchanger separates most of the tar compounds from the producer gas by condensing the heavier compounds (solid at atmospheric conditions) with a relatively high boiling point. The production of tars is approximately  $0.3 \text{ g}\cdot\text{m}^{-3}$ . The producer gas is combusted in the internal combustion engine (Ashok Leyland, India) with a 12:1 compression rate. Thus, the unit generates electrical energy and heat and solid biochar material with a high carbon content<sup>[25]</sup>. The exhaust gas delivers heat to the upper part of the gasifier in order to evaporate the remaining moisture from the feedstock.

The fuel and oxidising media (atmospheric air in this case) flows define this reactor as a so-called downdraft application. The reactor works in an autothermal regime. As a result, the lower heating value (LHV) parameter of the producer gas is relatively lower due to the presence of  $\text{CO}_2$  (combustion product) and  $\text{N}_2$  (from the atmospheric air). On the other hand, the energy necessary for the thermochemical reactions within the gasification reactor is not generated by any outer sources. The producer gas temperature ranges from 250 to 400 °C, and when appropriately cooled, the unit can generate up to 2  $\text{kW}_t$  per 1  $\text{kW}_e$ . According to the manufacturer, the unit can operate continuously for up to 16 h. A schematic of the PP 30 gasifier is shown in Figure 1 and a picture of the unit is presented in Figure 2.

### Experimental parameters

The experimental gasification process was held under a relatively low-load regime with softwood chips of 10-25 mm particle size. The equivalence ratio (ER) was as low as 0.22-0.25, whereas the fuel flow was equal to  $20 \text{ kg}\cdot\text{h}^{-1}$ . The average gasification temperature during the experimental measurement was between 850 and 900 °C. The pressure within the reactor was slightly below the atmospheric value to provide the flow of the gaseous products. The start-up time was 15 min because it was necessary to increase the temperature in the grate area above the desired gasification value (autothermal condition).

The efficiency of electricity production  $\eta_e$  was calculated based on

$$\eta_e = \frac{3.6P_e}{\dot{Q}_f \times LHV_f} \quad (1)$$

where  $P_e$ : representing the electric power in [kW];  $\dot{Q}_f$ : denoting the fuel flow in [ $\text{kg}\cdot\text{h}^{-1}$ ];  $LHV_f$ : indicating the fuel LHV in [ $\text{MJ}\cdot\text{kg}^{-1}$ ].

### Biochar analyses

The biochar was collected from a drop zone after the termination of the experimental operation. The subsequent analyses included ultimate and proximate analyses, along with LHV and pH value determinations. The contents of C, H, N and S were determined in the accredited Fuel laboratory of the Energy Research Centre, VSB - Technical University of Ostrava, Czech Republic. A CHNS628 (Leco, USA), along with the CHNS628S module, was used for this determination. The amount of O was calculated following the EN 16993 standard. The water content was determined using a gravimetric principle using a VF110 electric furnace (Mettler, Germany). Ash content was determined in an LE 05/11 furnace (LAC, Czech Republic). The higher heating value (HHV) was determined in an isoperibolic calorimetric pressure vessel HC600 (Leco, USA). The LHV parameter was determined as follows:

$$LHV = [HHV^d - 212.2w(H)^d - 0.8[w(O)^d + w(N)^d]] \times (1 - 0.01M) - 24.43M \quad (2)$$

where  $HHV^d$ : indicating HHV at a constant volume of the fuel in a dry state;  $w(H)^d$ : meaning the mass percentage of hydrogen;  $w(O)^d$ : representing the mass percentage of oxygen;  $w(N)^d$ : denoting the mass percentage of nitrogen;  $M$ : stands for the mass percentage of moisture.

The pH value was determined in accordance with the colourimetric method (ISO 10523:2008) for pH level determination using selective indicator papers (Lach:ner, Czech Republic) with a detection range from 6.0 to 7.5. The observed material was examined as a water solvent diluted for 24 h prior to the pH level measurement. The examination took 1 s and was compared to the standard scale in accordance with the manufacturer's manual.

### Biochar activation

Subsequently, the obtained biochar was subjected to a steam activation process at 850 °C. Steam activation was performed in a semi-batch vertical quartz reactor at 850 °C with a residence time of 25 min, using 1 g samples. The gasification process of biochar was conducted under a steam atmosphere (a mixture of heated to 300 °C  $H_2O$  and  $N_2$ ) at 850 °C. Details on the research rig and activation procedure can be found in the work of Mlonka-Mędrala *et al.* [26].

The gaseous phase collected during the activation process was analysed using a gas chromatography system, Agilent Technology 7890A GC. Gases such as  $CH_4$ ,  $CO_2$ ,  $O_2$ ,  $CO$ ,  $C_2H_6$ ,  $C_2H_4$ ,  $C_2H_2$  and  $H_2$  were detected at various concentrations.

Sample morphology and chemical composition were determined using a scanning electron microscope (SEM) equipped with energy-dispersive X-ray Nova NanoSEM 450 (Thermo Fisher Scientific Inc., USA) to identify the chemical composition of the samples. A 2 kV beam acceleration voltage was used for activated carbon morphology testing.

Fourier Transform Infrared Spectroscopy (FTIR) was employed to analyse the functional groups of the samples prior to and following the steam activation process. In the analyses conducted, the Bruker Alpha II instrument was employed to analyse the collected spectra in the range of 400 to 4,000  $cm^{-1}$ .

Further on, structural properties were determined using a gas adsorption method and ASAP 2020 volumetric analyser (Micromeritics, USA). The Brunauer-Emmet-Teller (BET) method was used to determine the specific surface area ( $S_{BET}$ ) of the activated carbons and the average diameter ( $D_p$ ) of the pores based on the adsorption isotherms with  $p/p_0$  ranging between 0.06 and 0.20; both adsorption and desorption curves were used. In the pore diameter measurement, the presence of the adsorbed layer was also included.

### Methanol sorption properties

Finally, to assess the potential of the produced porous carbon materials in adsorption cooling devices, methanol sorption properties were examined using a dynamic gravity vacuum system (DVS Vacuum). Based on experimental results, the adsorption and desorption isotherms were calculated. The methanol intake for all samples was determined depending on their saturation pressure. The materials were examined at two process temperatures, 30 and 60 °C, following previous studies which indicated that the temperature does not significantly influence the sorption properties of the activated carbons.

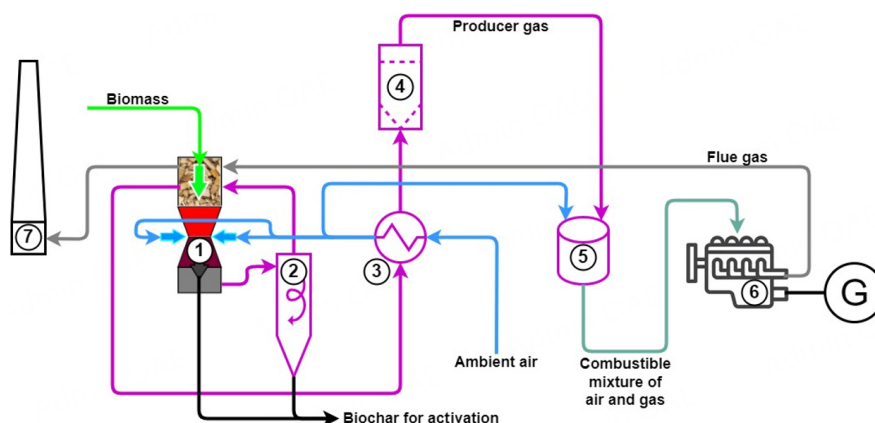


Figure 1. Scheme of the PP 30 gasification unit.

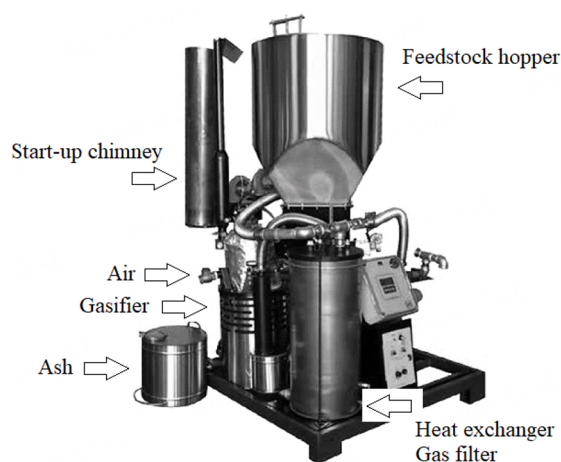


Figure 2. PP 30 gasification unit.

## RESULTS AND DISCUSSION

### Gasification process

The setup of the gasification technology provided a stabilised production of the gas for the piston combustion engine. The amount was roughly equal to  $15 \text{ m}^3 \cdot \text{h}^{-1}$ . This gas was sampled before being combusted and analysed separately (after the 30-min start-up and stabilisation period). Its parameters are summarised in Table 1. The gasification process was held at a reaction temperature of around  $790^\circ\text{C}$  while the starting temperature (combustion temperature before the process switched from combustion to gasification with a consequent temperature drop) reached  $890^\circ\text{C}$ . The obtained producer gas was composed of abundant CO ( $22\%_{\text{vol.}}$ ) and  $\text{H}_2$  ( $20\%_{\text{vol.}}$ ), which is beneficial from the combustion perspective. Despite the relatively high content of  $\text{N}_2$  ( $45\%_{\text{vol.}}$ ), the  $\text{LHV} = 6.31 \text{ MJ} \cdot \text{m}^{-3}$  is sufficient and very promising compared to similar studies on fixed bed downdraft<sup>[27,28]</sup> or cross-draft<sup>[29]</sup> gasification reactors. This might be due to very effective fuel conversion within the grate area, the result of which leaves the producer gas lacking tar compounds, generally diminishing its LHV after separation. The presence of  $\text{CO}_2$  is a natural consequence of the partial combustion of the fuel in autothermal applications, where no external heating is required. The combustion of this gas provided, in consequence, stable electricity production of  $27 \text{ kW}_e$ . Following Eq. 1, the electrical efficiency was equal to 29.6%. By a rough estimation, the price for the electricity was set to be 0.06 USD/kWh, when a potentially higher feedstock price was applied. The economy of the system could be



**Table 1. Composition and heating value of the producer gas**

Gasification process	CO % <sub>vol.</sub>	CH <sub>4</sub> % <sub>vol.</sub>	H <sub>2</sub> % <sub>vol.</sub>	CO <sub>2</sub> % <sub>vol.</sub>	N <sub>2</sub> % <sub>vol.</sub>	O <sub>2</sub> % <sub>vol.</sub>	LHV MJ·m <sup>-3</sup>	H <sub>2</sub> /CO	H <sub>2</sub> /CO <sub>2</sub>	Ref.
APL (downdraft), wood chips, air, ER = 0.22-0.25	22.0	3.0	20.0	10.0	45.0	0.0	6.31	0.91	2.00	this work
Entrained flow gasification (120 kW <sub>in</sub> ) torrefied wood, O <sub>2</sub> + steam, ER = 0.5	30.3	0.5	22.2	9.4	34.4	0.2	-	0.73	2.36	[34]
PRAGA gasifier (updraft), lignin A, 776 °C, air, ER = 0.17	24.8	3.0	26.0	9.5	36.4	0.2	7.30	1.05	2.74	[36]
PRAGA gasifier (updraft), lignin B, 687 °C, air, ER = 0.18	28.0	5.1	20.1	7.7	38.7	0.2	7.80	0.72	2.61	
LTB gasifier (downdraft), wood chips (moisture c. 11.6%), air, ER = 0.31	24.3	0.5	15.8	7.1	52.0	0.2	4.96	0.65	2.23	[35]
LTB gasifier (downdraft), wood pellets (moisture c. 9.5%), air, ER = 0.13	16.6	3.5	23.8	9.8	46.0	0.2	5.95	1.43	2.43	

further enhanced if the flue gas from the combustion process was introduced in a small-scale Organic Rankine Cycle (ORC) system, utilising a micro-scale turbine solution<sup>[30]</sup>.

Moreover, relatively low concentrations of CO<sub>2</sub> in the obtained gas seem to be favourable in terms of the use of such syngas in fermentation processes for the synthesis of different compounds. According to Rückel *et al.*<sup>[31]</sup>, the production of acetate by fermentation of syngas in a bubble column or gas-lift bioreactor using *Clostridia* is optimal when H<sub>2</sub>/CO and H<sub>2</sub>/CO<sub>2</sub> ratios are 1:1 and 2:1, respectively. Pacheco *et al.* obtained 51.1 mM of acetic acid and 2.0 mM of butyric acid after fermentation of syngas consisting of 24.2%<sub>vol.</sub> CO, 16.5%<sub>vol.</sub> CO<sub>2</sub>, and 23.9%<sub>vol.</sub> H<sub>2</sub>, using *Butyribacterium methylophilicum* strain<sup>[32]</sup>. The literature emphasises the relatively high tolerance of such microorganisms for tars in general<sup>[32]</sup>, as well as benzene, toluene, and xylene specifically<sup>[33]</sup>. Rückel *et al.* even reported that some impurities often found in syngas, such as NH<sub>3</sub> or H<sub>2</sub>S, can have a positive effect on both growth and alcohol formation during the fermentation process<sup>[34]</sup>. Results from other studies on gasification using different pilot/commercial scale gasifiers [Table 1] show that the gas obtained within the scope of this study is particularly well suited for subsequent fermentation, taking the aforementioned ideal proportions of H<sub>2</sub>/CO and H<sub>2</sub>/CO<sub>2</sub> into account. The obtained ratio H<sub>2</sub>/CO (this study) was only slightly worse than for the gasification of lignin in an updraft gasifier at 687 °C, whereas H<sub>2</sub>/CO<sub>2</sub> obtained within the scope of this study could be considered close to ideal, which was not the case for other studies, which all had ERs higher than 2. Among the results presented in Table 1, the closest to the ideal H<sub>2</sub>/CO<sub>2</sub> ratio equal to 2.31 was achieved for the low-tar biomass (LTB) gasifier (downdraft), gasification of wood chips (moisture 11.6%<sub>wt.</sub>), using air as a gasifying agent (ER = 0.31) in a custom-built downdraft LTB gasifier, designed by Technical University of Denmark (DTU), Denmark<sup>[35]</sup>. However, in this particular case, a relatively good H<sub>2</sub>/CO<sub>2</sub> ratio was accompanied by a suboptimal H<sub>2</sub>/CO ratio of 0.65.

Results presented in Table 1 clearly show that in many cases, low ER is favourable in terms of achieving relatively high LHV values. This could be easily explained by the fact that relatively low ER in air gasification results in a lower proportion between the feedstock and nitrogen in the gasifying agent (air), which in turn results in a producer gas with relatively small concentrations of N<sub>2</sub>.

Such a hypothesis is also supported by results of steam gasification, reported by Rückel *et al.*, which reported  $N_2$  in the gas<sup>[34]</sup>, but only because  $N_2$  was used for feeding the pulverised fuel. It seems important to highlight that  $LHV > 7 \text{ MJ}\cdot\text{m}^{-3}$  was achieved for the case in which air gasification was accompanied by the addition of steam<sup>[36]</sup>. Nonetheless, an increase in ER coincides with  $LHV < 7 \text{ MJ}\cdot\text{m}^{-3}$  [Table 1]. Care should be taken if the use of the producer gas for energy generation is considered, as gasification at low ER might be problematic from the point of view of heavy tars, as reported by Čespiva *et al.*<sup>[37]</sup>. However, the aforementioned tolerance of syngas fermentation for tars makes the issue less severe for such application of the obtained gas. Nonetheless, the composition of tars may vary due to many factors, such as ER, feedstock, temperatures in the gasifier, *etc.*<sup>[37]</sup>. Thus, it seems prudent to recommend more extensive research on the inhibition of syngas fermentation processes by tars from different types of gasifiers, operating using distinct feedstocks and ranges of process parameters.

It should not be overlooked that an increase in LHV of the gas might not necessarily mean a rise in the gasification efficiency since gasification at low ER can often be associated with significant yields of biochar chips<sup>[11]</sup>. This increases the loss in unconverted carbon, thus decreasing the process efficiency. However, it is meaningful only for the cases in which gasification is performed to produce gas for subsequent combustion as the only product. Polygeneration installations, which aim to produce biochar as one of the products, would not be affected by such an issue unless the produced biochar is not suitable for subsequent use.

### Biochar activation

The carbonaceous biochar derived from the gasification of wood chips was analysed in accordance with the abovementioned procedure. The individual particles suffered a 40%<sub>wt.</sub> weight loss (average gravimetric difference of the individual particles), and the C content within these was equal to 70.13%<sub>wt.</sub>.

Table 2 depicts the results of the ultimate and proximate analyses, where data from the raw material analyses are included for comparison. The pH of the samples was determined to be 6.8 on the pH scale - very slightly acidic, which is beneficial from the soil amendment point of view, as one of the possible applications of similar materials studied by Hansen *et al.* had proved<sup>[18]</sup>.

From Table 2, it is evident that the bulk density of the biomass material changed from 190 to 320  $\text{kg}\cdot\text{m}^{-3}$  after the gasification process, along with an increased  $LHV$  parameter (16.43 to 25.11  $\text{MJ}\cdot\text{kg}^{-1}$ ), which is attributed to the higher carbon content per kilogram (44.91 to 70.13%<sub>wt.</sub>). This can be considered beneficial from the material transport point of view. Referring to the energy density and content transported, the gasified material requires 61.1% less space for the same energy delivered (8,035.2 vs. 3,121.7  $\text{MJ}\cdot\text{m}^{-3}$ ). In other words, two trucks loaded with gasified material must have been replaced by five trucks in order to deliver the same amount of energy in raw material. The significance to the operating business economy is evident.

In order to further enhance the quality of the obtained biochar, a steam activation was performed to develop the porosity of the material. However, to minimise the generated waste and enhance the energy efficiency of the process, high-quality off-gas was collected during the activation process.

Characterisation of the material after steam activation is shown in Table 3, along with literature results presenting different biochars and activated carbons used as sorbents.

In the presented study, activated biochar was characterised by noticeable  $S_{BET} = 565.87 \text{ m}^2\cdot\text{g}^{-1}$ , noticeable micropore volume equal to  $0.227 \text{ cm}^3\cdot\text{g}^{-1}$ , and pore size equal to 2.12 nm. It seems that the obtained



**Table 2. Activated carbon characteristics**

Parameter	Symbol	Unit	Value		Standard
			Raw <sup>r</sup>	Gasified <sup>d</sup>	
Water	W	% <sub>wt.</sub>	9.38	0	ISO 181234-2
Ash	A	% <sub>wt.</sub>	0.93	9.74	ISO 18122
Carbon	C	% <sub>wt.</sub>	44.91	70.13	ISO 16948
Hydrogen	H	% <sub>wt.</sub>	5.34	3.08	ISO 16948
Nitrogen	N	% <sub>wt.</sub>	0.21	1.25	ISO 16948
Sulphur	S	% <sub>wt.</sub>	0.02	0.05	ISO 16994
Oxygen	O	% <sub>wt.</sub>	39.21	15.75	ISO 16993
Lower heating value	LHV	MJ·kg <sup>-1</sup>	16.43	25.11	ISO 18125
Higher heating value	HHV	MJ·kg <sup>-1</sup>	17.82	25.77	ISO 18125
Potential of hydrogen	pH	-	-	6.8	ISO 10523:2008

<sup>r</sup>raw; <sup>d</sup>dry.

activated carbon has similar properties to some commercial activated carbons obtained using physical methods, such as Norit GL 50 ( $S_{BET} = 580.23 \text{ m}^2\cdot\text{g}^{-1}$ ) produced by Cabot Corporation or AKPA-22 ( $S_{BET} = 750.66 \text{ m}^2\cdot\text{g}^{-1}$ ) produced by Gryfskand, which makes this material a good sustainable alternation on the market. Also, similar material was studied in the acquisition of the LCA (Life Cycle Assessment) application, pointing out the promising impact of biochar and char production<sup>[40]</sup>.

Apart from moderately high surface area, when compared to commercially available activated carbons, activated carbons obtained within the scope of this study could become good sorbents. Marchelli *et al.* successfully used sorbents of similar (and in some cases worse) surface area, pore diameter, and volume to effectively remove H<sub>2</sub>S from model syngas<sup>[38]</sup>. Moreover, sorbents used by Marchelli *et al.* were also by-products from the gasification of wood<sup>[38]</sup>. This shows that a part of the biochar stream can successfully be utilised for its own needs of gasification installation. Additionally, gasification installations producing such sorbents could find local customers in rural areas, as H<sub>2</sub>S is also a problem for installations producing biogas by anaerobic digestion<sup>[41,42]</sup>. In such case, lower sorption capacity, in comparison to commercial activated carbons, should not be considered a problem since the local source of such sorbent allows a substantial decrease in transportation costs. Thus, lower sorption capacity could be compensated by a larger size of the adsorbent bed or a more frequent change of the sorbent.

Physical activation performed within the scope of this study resulted in a relatively well-developed surface, comparable to other methods of physical activation, such as using CO<sub>2</sub> [Table 3]. Kilpimaa *et al.* reported that physical activation was sufficient to produce adsorbents for the removal of phosphates and nitrates in wastewater treatment<sup>[39]</sup>. Moreover, the same authors considered such sorbents as a low-cost alternative to commercial activated carbons in terms of phosphate removal. It should not be overlooked that the activated carbons produced within the scope of this study required a relatively shorter residence time (25 min) and only a slightly higher temperature (850 °C) compared to the physical activation performed by Kilpimaa *et al.*, resulting in a fairly similar BET surface area [Table 3]<sup>[39]</sup>. This is promising, as lower residence time effectively means a smaller size of the reactor or higher productivity for comparable reactors for physical activation. Nonetheless, it should not be overlooked that apart from physical sorption, chemisorption may also play a significant role in such applications. Therefore, a detailed analysis of functional groups on the surface of the produced activated carbons should always accompany porosimetry and assessment of the morphology before any meaningful conclusions can be drawn. Based on FTIR spectra of raw biochar and biochar obtained after activation presented in Figure 3, functional groups

**Table 3. Comparison of different activated carbons**

Preparation of biochar/activated carbon	BET surface area, m <sup>2</sup> ·g <sup>-1</sup>	Average pore diameter, nm	Pore volume, cm <sup>3</sup> ·g <sup>-1</sup>	Content, % <sub>dry</sub>	Ref.
Downdraft gasifier (850-900 °C); air - ER between 0.22 and 0.25; softwood chips of 10-25 mm particle size, fuel flow rate 20 kg·h <sup>-1</sup> + subsequent activation with steam.	565.87	2.12	0.23	70.13	This study
Downdraft gasifier (1,073 K); air; wood chips	281.23	5.22	0.23	80.64	
Rising co-current gasifier (973 K); air; wood chips	127.67	7.08	0.28	80.23	[38]
Downdraft gasifier (1,073 K); air; wood chips (different gasifier)	77.90	8.58	0.08	48.12	
Spouting bed gasifier (1,153-1,173 K); air; wood pellets	103.97	5.18	0.14	49.90	[39]
Dual stage (1,173 K); air; wood chips	586.72	3.88	0.30	78.09	
Commercial activated carbons	1,002-1,269	5.20-6.10	0.51-0.91	90.65-82.42	[39]
150 kW downdraft gasifier (1,000 °C); wood chips (forestry in Finland); physical activation, CO <sub>2</sub> , 600 °C, 1 h	150	5.25	0.196	-	
150 kW downdraft gasifier (1,000 °C); air; wood chips (forestry in Finland); physical activation, CO <sub>2</sub> , 600 °C, 3 h	152	5.20	0.197	-	
150 kW downdraft gasifier (1,000 °C); air; wood chips (forestry in Finland); physical activation, CO <sub>2</sub> , 800 °C, 1 h	353	3.86	0.340	-	
150 kW downdraft gasifier (1,000 °C); air; wood chips (forestry in Finland); physical activation, CO <sub>2</sub> , 800 °C, 3 h	590	3.44	0.335	-	

ER: Equivalence ratio.

transformation during steam activation were discussed. It should be noted that carbon content is not always correlated with surface area, average pore diameter and volume [Table 3].

The surface of the char was examined in order to identify the specific chemical bonds present in the samples. The spectra of biochar and biochar after steam activation are presented in Figure 3. For activated biochar, relatively weak absorption at wavenumbers from 2,800 cm<sup>-1</sup> up to 4,000 cm<sup>-1</sup> is noted. In the case of raw biochar, the same situation occurred for wavenumbers from 2,500 cm<sup>-1</sup> up to 4,000 cm<sup>-1</sup>. This phenomenon can suggest that studied samples exhibited minimal quantities of hydroxyl groups or aliphatic structures<sup>[43]</sup>. Peaks from the area of 2,600-2,800 cm<sup>-1</sup> could be associated with C-H bending motions, while lower peaks correspond mainly to C-O various bonds of aromatic structures<sup>[44]</sup>. The adsorption region of 900-1,300 cm<sup>-1</sup> in the case of biochar displays an increase, while in the case of activated biochar, it appears in trace of those bounds from the sample before activation. This region is associated with the overlapping single vibrations of C-O bonds in different forms, such as ethers and esters, as well as the char carbonaceous matrix of C-C bonds<sup>[44]</sup>. Peaks presented at 1,424 cm<sup>-1</sup> are usually associated to the variable-angle vibration of C-OH<sup>[45]</sup>. A decrease in the peak at 1,424 cm<sup>-1</sup> indicates the release of -CH<sub>3</sub> from alkanes, and -CH<sub>3</sub> detached radicals or small molecules are released into the gas phase<sup>[46]</sup>. Peak 1,576 cm<sup>-1</sup> disappears after activation due to the breakdown of C=C<sup>[47]</sup>. The last of the highest peaks at 874 cm<sup>-1</sup> for raw biochar indicates a single dominant substitution pattern in aromatic structures, whereby only one or two adjacent H atoms bonded to the ring are involved<sup>[46]</sup>. The reduction of peaks observed between 750 and 880 cm<sup>-1</sup>, in the case of the activated biochar, is indicative of the removal of H radicals, which in turn leads to the formation of small molecules such as H<sub>2</sub>, CH<sub>4</sub> and other hydrocarbons. During pyrolysis,

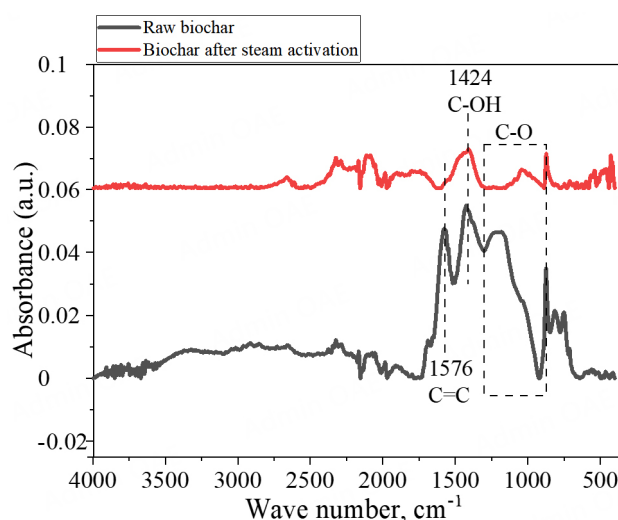


**Figure 3.** FTIR spectra of raw biochar and biochar obtained after steam activation.

biomass can be considered a donor of H radicals<sup>[48]</sup>, which is also relevant from the point of view of the gasification process due to the existence of a pyrolysis zone in fixed-bed gasifiers. Jiang *et al.* have shown that during the pyrolysis of lignin the alkyl side chain and characteristic functional groups can donate H for methyl radicals to form methane<sup>[49]</sup>. This is possible due to the homolytic cleavage of H from the monomers of lignin<sup>[49]</sup>. Similarly, a reduction in the adsorption capacity of biochar following steam activation suggests the disruption of bonds present in the material before activation, resulting in the solid material conversion into syngas.

The off-gas analysis is presented in Table 4 ( $N_2$  content was excluded in the calculations as it comes from the reactor construction, and in a large-scale process, this could be minimised). It should be noted that the production of steam using producer gas and off-gas from activation could be beneficial from the point of view of the energy balance of such an installation. Moreover, as far as fermentation of syngas is considered, a part of the off-gas from activation could be mixed with the gas from gasification in order to make  $H_2/CO$  of the mixture closer to ideal ( $H_2/CO = 2.0$ ) when compared with the gas from gasification on its own [Table 2].

The off-gas, obtained during the activation step, was characterised by a very high content of  $H_2$  and CO, but a low content of  $CO_2$  was measured as well. Therefore, the yield of  $H_2$  and CO is most likely related to the steam gasification of carbon ( $C + H_2O \rightarrow CO + 3H_2$ ). The fact that the content of  $CO_2$  was relatively small can also be considered beneficial, as it is an inert gas that decreases the LHV of the produced syngas. The off-gas obtained within the scope of this study was similar to the off-gas obtained by Hwang *et al.* during KOH activation [Table 4] for the case of solid-solid mixing<sup>[50]</sup>. On the other hand, off-gas obtained by these authors during KOH activation with wet impregnation had much lower concentrations of  $H_2$ , and much higher concentrations of CO and  $CO_2$ .

Looking from the point of view of using syngas for electricity generation, since the majority of the compounds in the off-gas are combustible [Table 3], mixing them with syngas after condensation of remaining steam and before the carburettor, where the producer gas is mixed with air, seems reasonable. On the one hand, this could increase the fire and explosion risk, which is non-negligible for a producer gas from the biomass gasification process, as reported by Zhou *et al.*<sup>[51]</sup> or Skřínský *et al.*<sup>[52]</sup>. On the other hand,

**Table 4. Analysis of the off-gas from the steam activation process**

Activation process	CH <sub>4</sub> % <sub>vol.</sub>	C <sub>2</sub> H <sub>6</sub> % <sub>vol.</sub>	C <sub>2</sub> H <sub>2</sub> % <sub>vol.</sub>	H <sub>2</sub> % <sub>vol.</sub>	CO <sub>2</sub> % <sub>vol.</sub>	O <sub>2</sub> % <sub>vol.</sub>	CO % <sub>vol.</sub>	LHV MJ·m <sup>-3</sup>	Ref.
Steam activation, 850 °C, 25 min	4.52	0.08	0.50	70.40	3.42	0.17	20.92	11.58	This study
KOH activation, K/C = 0.2 (mol/mol); solid-solid mixing	1.65	n.d.	n.d.	71.51	7.07	n.d.	19.77	10.26	
KOH activation, K/C = 0.3 (mol/mol); solid-solid mixing	4.73	n.d.	n.d.	80.13	1.47	n.d.	13.67	11.46	
KOH activation, K/C = 0.5 (mol/mol); solid-solid mixing	6.23	n.d.	n.d.	81.19	0.16	n.d.	12.41	11.93	[50]
KOH activation, K/C = 0.2 (mol/mol); wet impregnation	0.31	n.d.	n.d.	31.07	34.77	n.d.	33.85	7.36	
KOH activation, K/C = 0.3 (mol/mol); wet impregnation	0.15	n.d.	n.d.	23.02	42.53	n.d.	34.30	6.54	
KOH activation, K/C = 0.5 (mol/mol); wet impregnation	0.00	n.d.	n.d.	32.96	20.99	n.d.	46.05	8.92	

Literature results recalculated from Hwang et al.<sup>[50]</sup> from mmol/mmolAC, based on the assumption that the gas consisted only of CH<sub>4</sub>, H<sub>2</sub>, CO<sub>2</sub>, and CO, assuming heating values of 33.906, 10.246, and 12.035 MJ/m<sup>3</sup> for CH<sub>4</sub>, H<sub>2</sub>, and CO, respectively; n.d.: not determined.

particulate matter is removed from the gas prior to mixing with air, thus minimising the risk of static electricity causing sparks in a potentially explosible mixture. The addition of the off-gas into the synthetic gas would result in higher LHV of the mixture compared to the syngas. Moreover, a reduction of the CO<sub>2</sub> content due to the relatively low CO<sub>2</sub> concentration of the off-gas (3.42%<sub>vol.</sub>) could be expected, which is crucial considering the challenging decarbonisation goals in the energy sector.

The addition of such an off-gas to the producer gas would certainly influence the combustion process itself. Shivapuji and Dasappa<sup>[53]</sup> observed that an increase in the hydrogen fraction above 11%<sub>vol.</sub> made syngas exceed laminar burning speeds of methane. On the other hand, increasing concentration of H<sub>2</sub> in syngas resulted in increased cooling need of the engine<sup>[53]</sup>, which could be perceived both as a complication (changes in engine cooling requirement) and as an opportunity (heat recovered from engine cooling could be subsequently used for heating purposes). Solferini de Carvalho et al. observed during the experimental investigation on the combustion of producer gas in a spark ignition engine that the 33%<sub>vol.</sub> of H<sub>2</sub> in producer gas improved the flame morphology of the mixture, making it resemble that of pure natural gas<sup>[54]</sup>.

The influence of steam activation on the biochar morphology was determined based on analysis of the activated and non-activated biochar. The resulting images of morphology are shown in Figure 4.

In the case of lignocellulosic materials, a very well-developed porous structure is usually obtained. In addition, the presented study also showed that a regular pore structure was observed with characteristics of homogeneous materials, very similar to the morphology of activated carbons derived from biomass wastes<sup>[16]</sup>. Spherical particles of the mineral phase are also present in the photograph. These are directly responsible for lowering the active surface area of the material. However, in the case of materials obtained from wood biomass, the ash content is usually negligible. Thus, high values of the internal surface should be expected, which was confirmed by tests carried out using low-temperature gas adsorption. The observed chemical transformations in the activated biochar can be primarily associated with changes within specific functional groups that are directly related to the steam activation process. The FTIR spectra [Figure 3] reveal a reduction in absorption in the 2,800-4,000 cm<sup>-1</sup> range for both the raw and activated biochar samples. This phenomenon suggests a reduction in hydroxyl groups and aliphatic structures<sup>[43]</sup>. The steam activation process favours the decomposition of these structures<sup>[55]</sup>. Furthermore, the FTIR peak at 1,424 cm<sup>-1</sup> provides additional evidence that the steam activation process results in the breakdown of alkyl chains and other functional groups due to the release of -CH<sub>3</sub> release from alkanes. The reduction in peaks from the 750 and 880 cm<sup>-1</sup> spectra is associated with aromatic structures due to the formation of small molecules such as H<sub>2</sub> and CH<sub>4</sub>, which are crucial in syngas production<sup>[55]</sup>. Furthermore, the process of steam

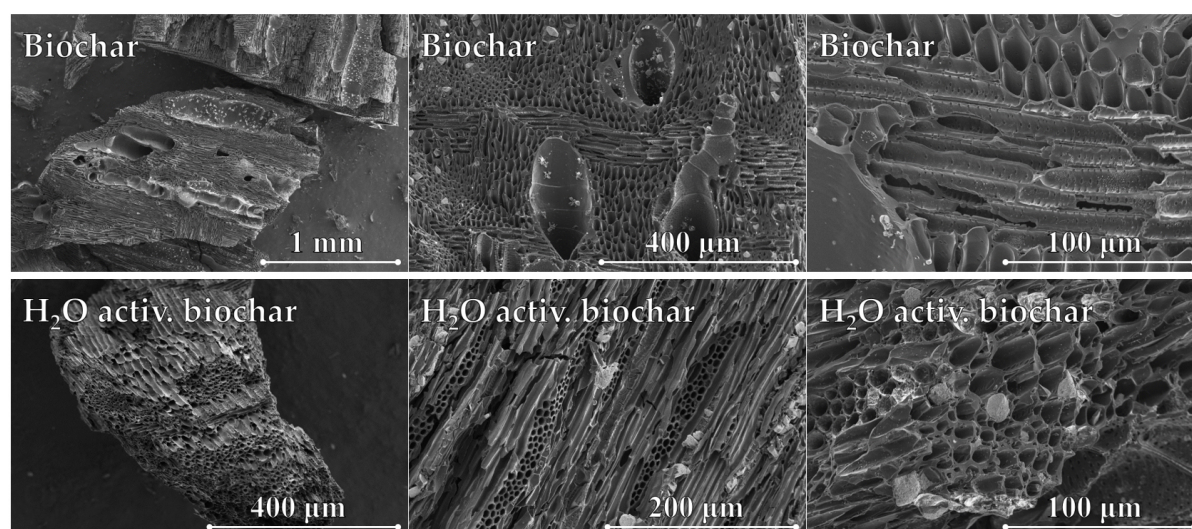


**Figure 4.** Sample morphology for raw biochar and biochar obtained after steam activation.

activation has a considerable effect on the surface structure of biochar. Prior to activation, biochar derived from lignocellulosic materials typically exhibits a well-developed porous structure<sup>[56]</sup>. Following the activation process, the structure becomes more notable, similar to that observed in activated carbons derived from biomass, as evidenced by the conducted low-temperature gas adsorption analysis<sup>[57]</sup>. The presence of mineral phase particles, despite reducing the overall active surface area, is minimal in biochar derived from wood biomass due to its low ash content<sup>[58]</sup>. The relationship between chemical bond disruption and morphological alterations is a crucial aspect of understanding the transformation of biochar during steam activation.

The elemental mapping results for raw biochar and biochar obtained after steam activation are evident in [Figure 5](#).

Based on elemental mapping performed for both raw and steam-activated biochar, it appears that raw biochar was contaminated with KCl salt, which might limit the potential use of the produced biochar in the energy sector due to possible issues related to alkali salts such as fouling, agglomeration, and high-temperature corrosion<sup>[59–61]</sup>. However, further steam activation favours the release of inorganic salts<sup>[62]</sup>, which could be beneficial from the point of view of increasing the specific surface of particles since such deposits could potentially block some of the pores, as shown in [Figure 4](#). On the other hand, this might indicate that cooling of the off-gases might require special attention due to the possibility of alkali salt deposits being formed at cool surfaces. Further research on this aspect is recommended.

The mineral matter of the activated biochar is composed mainly of CaO, which is also a characteristic of wood biomass<sup>[63]</sup>.

### Methanol sorption

Dynamic vapour adsorption tests showed that raw biochar was a stable porous carbon material with a limited adsorption capacity toward methanol. The amount of adsorbed methanol did not exceed  $0.9 \text{ kg}_{\text{MeOH}} \cdot \text{kg}^{-1}$  adsorbent. Whereas after the activation, the adsorption capacity almost doubled, but only at a temperature of 60 °C. However, at a given equilibrium pressure, the equilibrium adsorption capacity should decrease with increasing adsorbent temperature<sup>[64]</sup>. In our case, we can observe that at 60 °C, the adsorption



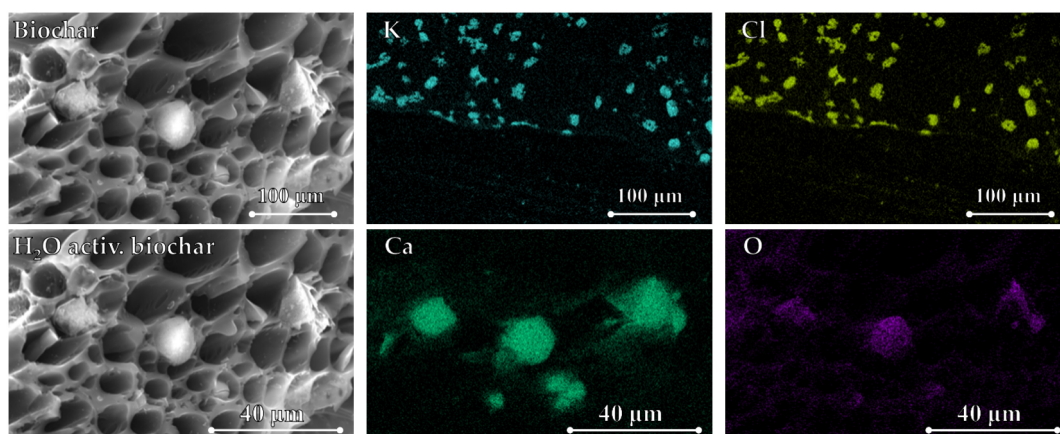


**Figure 5.** Elemental mapping results for raw biochar and biochar obtained after steam activation.

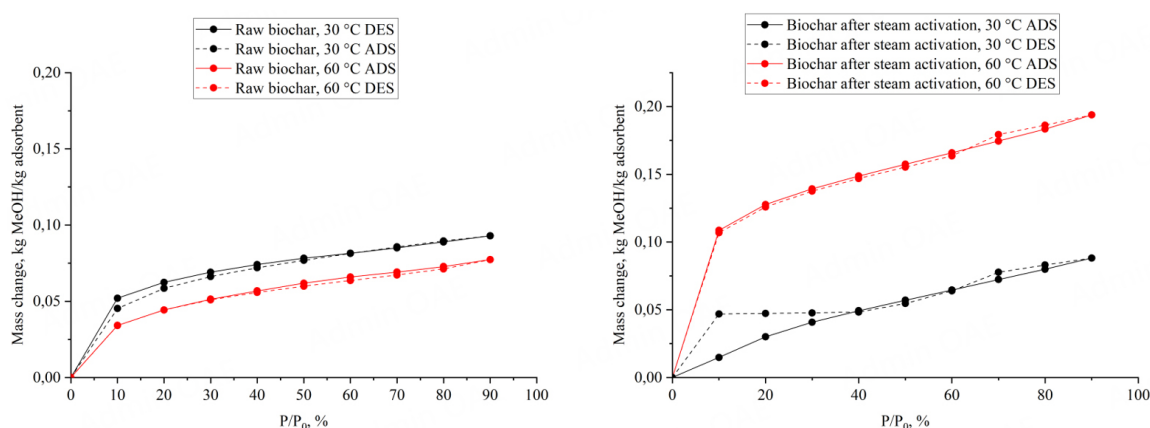


**Figure 6.** Adsorption and desorption isotherms for raw biochar and steam-activated biochar at 30 and 60 °C.

capacity is higher than at 30 °C. The anomaly observed in Figure 6 for steam-activated biochar might be explained by the unstable structure of the material analysed.

In our case, the adsorption capacity increased with temperature, indicating that the adsorption process was endothermic. Higher temperatures are known to enhance the diffusion rate of adsorbate molecules through the external boundary layer and into the internal pores of the adsorbent particles. This improvement in adsorption capacity may be attributed to chemical interactions between the adsorbent and adsorbate or the formation of new adsorption sites.

Both samples were characterised by a type I adsorption isotherm, and there was practically no hysteresis of adsorption, which confirms that the tested material has a microporous structure. However, slight H4-type hysteresis was observed in all temperatures analysed; it could be associated with the presence of split pores in the material. Microporous structure and an increase of adsorption capacity through steam activation are very promising, but the structure of the material needs to be enhanced to consider it as a potential bed material in an adsorption cooling device.



It should be emphasised that the chief advantage of the hereby-described technological process should be sought in its off-grid application, where managing the biowaste accumulation is often problematic<sup>[65]</sup>. Profitable ways are often hindered by location-specific, multidisciplinary issues<sup>[66]</sup>, whereas efficient and sustainable production of universal bio-sorbents with a parallel production of affordable electricity (utilisable for the facility operation, including the activation processes) can increase the profit and protect the surrounding environment at the same time.

The sustainability and self-sufficiency of the examined device are reasonably satisfying, and the performance of electric energy generation from biomass waste material could be significant. Utilising another by-product from the technology will strengthen its market position and enhance the chances of achieving global decarbonisation goals, especially in remote and cut-off areas with access to obtainable biomass resources, optimally combined with intermittent energy sources, such as solar or wind. This will further support the goal of a sustainable and fossil-free society.

In the following studies, the focus on various bio-feedstock, including the marginal materials unsuitable for animal feed, would not be ill-placed as the operational variability of the PP 30 gasifier was not studied thoroughly, while the character of available waste biomass varies greatly around the globe.

## CONCLUSION

In this study, the performance of the commercially available PP 30 gasifier was determined from the energy and alternative carbonaceous material production points of view. It was found that this off-grid unit is capable of stable generation of electricity with a power of 27 kW<sub>e</sub>, additionally producing a sufficient amount of biochar, which, after steam activation, could be considered a marketable product. The C content within these produced solid residues was equal to 70.13%<sub>w</sub>. That makes this material suitable for numerous applications where a carbonaceous structure is of the essence, such as a sorption material or purification element. With  $LHV = 25.11 \text{ MJ}\cdot\text{kg}^{-1}$ , this material can be considered very interesting in terms of energy accumulation as well.

Steam activation allowed improvement in terms of the specific surface area of the biochar particles, with  $S_{BET} = 565.87 \text{ m}^2\cdot\text{g}^{-1}$  when standard physical activation is applied, making it an optimal material to replace fossil-based products in the field of air/flue gas/water purification or other applications, such as adsorption cooling techniques. Such material can help reduce transportation demand by 61.1% within the biomass fuel supply chain and, thus, significantly diminish the utilisation of fossil resources, both in production and transportation.

It seems plausible to recommend further work on such small-scale polygeneration systems in order to fully confirm their sustainability from both environmental and economic perspectives. Such research endeavours would include techno-economic analysis and life cycle assessment. Moreover, further research is recommended with respect to the behaviour of inorganics present in biochar during the activation process since the potential formation of deposits of alkali salts formed during activation might have a significant influence on the maintenance of such systems. More work is also needed on the inhibition of syngas fermentation processes by tars from various types of gasifiers operating using different feedstocks and ranges of process parameters. Furthermore, more studies on the economic feasibility of such polygeneration installations are needed.

## DECLARATIONS

### Authors' contributions

Conceptualisation, funding acquisition: Čespiva, J.; Mlonka-Mędrala, A.

Experimental acquisition (gasification): Čespiva, J.; Skřínský, J.; Jadlovec, M.; Výtisk, J.

Experimental acquisition (sorbent analysis and application): Mlonka-Mędrala, A.; Sieradzka, M.; Kalawa, W.; Sowa, M.

Data analysis: Čespiva, J.; Mlonka-Mędrala, A.; Niedźwiecki, L.; Wang, X.; Chen, W. H.

Manuscript preparation: Čespiva, J.; Mlonka-Mędrala, A.; Niedźwiecki, L.; Chen, W. H.; Thangavel, S.

Technical and material support: Čespiva, J.; Mlonka-Mędrala, A.; Skřínský, J.

### Availability of data and materials

The related data, deposited in the individual repositories of the participating institutions, will be provided upon request.

### Financial support and sponsorship

This work was co-financed by the Recovery and Resilience Facility within the National Centre for Energy II, reg. no. TN02000025, and by the European Union under the REFRESH Research Excellence For Region Sustainability and High-tech Industries project No CZ.10.03.01/00/22\_003/0000048 via the Operational Programme Just Transition. This work received funding from the European Union's Horizon 2020 Research and Innovation Programme under a Marie Skłodowska-Curie grant (No 823745) and was partly supported by program "Excellence initiative - research university" for the AGH University of Science and Technology and Polish Ministry of Science and Higher Education within the program "PMW" 2019-2022, grant no W48/H2020/2019 (grant agreement 5067/HORYZONT2020/2019/2).

### Conflicts of interest

All authors declared that there are no conflicts of interest.

### Ethical approval and consent to participate

Not applicable.

### Consent for publication

Not applicable.

### Copyright

© The Author(s) 2025.

## REFERENCES

1. Eurostat. EU's circular material use rate increased in 2020; 2021. Available from: <https://ec.europa.eu/eurostat/web/products-eurostat-news/-/ddn-20211125-1> [Last accessed on 15 Nov 2024].
2. Horák, J.; Kuboňová, L.; Hopan, F.; et al. Influence of co-combustion of unsuitable fuels with standardized fuels in households on CO, OGC, PM, and PAH emissions. *Environ. Sci. Pollut. Res. Int.* **2022**, 29, 44297-307. DOI
3. Ryšavý, J.; Horák, J.; Kuboňová, L.; et al. Beech leaves briquettes as fuel for a home combustion unit. 2020; pp. 75-85. Available from: [https://www.researchgate.net/profile/Jiri-Rysavy/publication/343427834\\_BEECH\\_LEAVES\\_BRIQUETTES\\_AS\\_FUEL\\_FOR\\_A\\_HOME\\_COMBUSTION\\_UNIT/links/5f7344b5a6fdcc00864672d1/BEECH-LEAVES-BRIQUETTES-AS-FUEL-FOR-A-HOME-COMBUSTION-UNIT.pdf?origin=scientificContributions](https://www.researchgate.net/profile/Jiri-Rysavy/publication/343427834_BEECH_LEAVES_BRIQUETTES_AS_FUEL_FOR_A_HOME_COMBUSTION_UNIT/links/5f7344b5a6fdcc00864672d1/BEECH-LEAVES-BRIQUETTES-AS-FUEL-FOR-A-HOME-COMBUSTION-UNIT.pdf?origin=scientificContributions) [Last accessed on 15 Nov 2024].
4. Pedrazzi, S.; Santunione, G.; Mustone, M.; et al. Techno-economic study of a small scale gasifier applied to an indoor hemp farm: from energy savings to biochar effects on productivity. *Energy. Convers. Manag.* **2021**, 228, 113645. DOI
5. Prakash, M.; Sarkar, A.; Sarkar, J.; Chakraborty, J. P.; Mondal, S. S.; Sahoo, R. R. Performance assessment of novel biomass gasification based CCHP systems integrated with syngas production. *Energy* **2019**, 167, 379-90. DOI
6. Prakash, M.; Sarkar, A.; Sarkar, J.; Mondal, S. S.; Chakraborty, J. P. Proposal and design of a new biomass based syngas production system integrated with combined heat and power generation. *Energy* **2017**, 133, 986-97. DOI

7. Pedrazzi, S.; Santunione, G.; Minarelli, A.; Allesina, G. Energy and biochar co-production from municipal green waste gasification: A model applied to a landfill in the north of Italy. *Energy. Convers. Manag.* **2019**, *187*, 274–82. DOI
8. Morselli, N.; Dalmonte, F.; Tartarini, P. Gasification as possible technological solution for driftwood management in bodies of waters. *IOP. Conf. Ser. Earth. Environ. Sci.* **2022**, *1106*, 012014. DOI
9. Merzic, A.; Turkovic, N.; Ikanovic, N.; Lapandic, E.; Kazagic, A.; Music, M. Towards just transition of coal regions - cultivation of short rotation copies and dedicated energy crops for biomass co-firing vs photo voltaic power plants. *Energy. Convers. Manag. X.* **2022**, *15*, 100267. DOI
10. Čespiva, J.; Jadlovec, M.; Výtisk, J.; Serenčíšová, J.; Tadeáš, O.; Honus, S. Softwood and solid recovered fuel gasification residual chars as sorbents for flue gas mercury capture. *Environ. Technol. Innov.* **2023**, *29*, 102970. DOI
11. Čespiva, J.; Niedzwiecki, L.; Wnukowski, M.; et al. Torrefaction and gasification of biomass for polygeneration: production of biochar and producer gas at low load conditions. *Energy. Rep.* **2022**, *8*, 134–44. DOI
12. Ryšavý, J.; Čespiva, J.; Kuboňová, L.; et al. Co-gasification of pistachio shells with wood pellets in a semi-industrial hybrid cross/updraft reactor for producer gas and biochar production. *Fire* **2024**, *7*, 87. DOI
13. Fajimi, L. I.; Oboirien, B. O.; Adams, T. A. Simulation studies on the co-production of syngas and activated carbon from waste tyre gasification using different reactor configurations. *Energy. Convers. Manag. X.* **2021**, *11*, 100105. DOI
14. Wystalska, K.; Malińska, K.; Barczak, M. Poultry manure derived biochars - the impact of pyrolysis temperature on selected properties and potentials for further modifications. *J. Sustain. Dev. Energy. Water. Environ. Syst.* **2021**, *9*, 1080337. DOI
15. Castiglioni, M.; Rivoira, L.; Ingrando, I.; et al. Biochars intended for water filtration: a comparative study with activated carbons of their physicochemical properties and removal efficiency towards neutral and anionic organic pollutants. *Chemosphere* **2022**, *288*, 132538. DOI
16. Sieradzka, M.; Mlonka-Mędrala, A.; Kalembe-Rec, I.; et al. Evaluation of physical and chemical properties of residue from gasification of biomass wastes. *Energies* **2022**, *15*, 3539. DOI
17. Mlonka-Mędrala, A.; Hasan, T.; Kalawa, W.; et al. Possibilities of using zeolites synthesized from fly ash in adsorption chillers. *Energies* **2022**, *15*, 7444. DOI
18. Hansen, V.; Müller-Stöver, D.; Ahrenfeldt, J.; Holm, J. K.; Henriksen, U. B.; Hauggaard-Nielsen, H. Gasification biochar as a valuable by-product for carbon sequestration and soil amendment. *Biomass. Bioenergy.* **2015**, *72*, 300–8. DOI
19. Santunione, G.; Turi, E.; Paris, R.; Francia, E.; Montanari, M.; Cannazza, G. Production and use of co-composted biochar as soil amendment for cannabis sativa sp. growth. 2020. pp. 113–7. Available from: <https://iris.unimore.it/handle/11380/1239367> [Last accessed on 15 Nov 2024].
20. Phuphuakrat, T.; Namioka, T.; Yoshikawa, K. Tar removal from biomass pyrolysis gas in two-step function of decomposition and adsorption. *Appl. Energy.* **2010**, *87*, 2203–11. DOI
21. Shen, Y. Chars as carbonaceous adsorbents/catalysts for tar elimination during biomass pyrolysis or gasification. *Renew. Sustain. Energy. Rev.* **2015**, *43*, 281–95. DOI
22. Sur, A.; Das, R. K. Experimental investigation on waste heat driven activated carbon-methanol adsorption cooling system. *J. Braz. Soc. Mech. Sci. Eng.* **2017**, *39*, 2735–46. DOI
23. Tchoffor, P. A.; Davidsson, K. O.; Thunman, H. Production of activated carbon within the dual fluidized bed gasification process. *Ind. Eng. Chem. Res.* **2015**, *54*, 3761–6. DOI
24. Gañán, J.; Turegano, J. P.; Calama, G.; Roman, S.; Al-Kassir, A. Plant for the production of activated carbon and electric power from the gases originated in gasification processes. *Fuel. Process. Technol.* **2006**, *87*, 117–22. DOI
25. Puglia, M.; Morselli, N.; Pedrazzi, S.; Tartarini, P.; Allesina, G.; Muscio, A. Specific and cumulative exhaust gas emissions in micro-scale generators fueled by syngas from biomass gasification. *Sustainability* **2021**, *13*, 3312. DOI
26. Mlonka-Mędrala, A.; Sieradzka, M.; Magdziarz, A. Thermal upgrading of hydrochar from anaerobic digestion of municipal solid waste organic fraction. *Fuel* **2022**, *324*, 124435. DOI
27. Vonk, G.; Piriou, B.; Felipe, D. S. P.; Wolbert, D.; Vähtilingom, G. Comparative analysis of wood and solid recovered fuels gasification in a downdraft fixed bed reactor. *Waste. Manag.* **2019**, *85*, 106–20. DOI
28. Susastriawan, A. A.; Saptoadi, H. Effect of air supply location and equivalence ratio on thermal performance of downdraft gasifier fed by wood sawdust. *J. Sustain. Dev. Energy. Water. Environ. Syst.* **2023**, *11*, 1100435. DOI
29. Čespiva, J.; Niedzwiecki, L.; Vereš, J.; et al. Evaluation of the performance of the cross/updraft type gasification technology with the sliding bed over a circular grate. *Biomass. Bioenergy.* **2022**, *167*, 106639. DOI
30. Kupka, D.; Koloničný, J. Design and experimental investigation of a micro-scale bladeless-type steam turbine. *Appl. Therm. Eng.* **2024**, *239*, 122119. DOI
31. Rückel, A.; Oppelt, A.; Leuter, P.; Johne, P.; Fendt, S.; Weuster-Botz, D. Conversion of syngas from entrained flow gasification of biogenic residues with *Clostridium carboxidivorans* and *Clostridium autoethanogenum*. *Fermentation* **2022**, *8*, 465. DOI
32. Pacheco, M.; Pinto, F.; Ortigueira, J.; Silva, C.; Gírio, F.; Moura, P. Lignin syngas bioconversion by *Butyrivibacterium methylotrophicum*: advancing towards an integrated biorefinery. *Energies* **2021**, *14*, 7124. DOI
33. Piatek, P.; Olsson, L.; Nygård, Y. Adaptation during propagation improves *Clostridium autoethanogenum* tolerance towards benzene, toluene and xylenes during gas fermentation. *Bioresour. Technol. Rep.* **2020**, *12*, 100564. DOI
34. Rückel, A.; Hannemann, J.; Maierhofer, C.; Fuchs, A.; Weuster-Botz, D. Studies on syngas fermentation with *Clostridium carboxidivorans* in stirred-tank reactors with defined gas impurities. *Front. Microbiol.* **2021**, *12*, 655390. DOI PubMed PMC

35. Rahman, M. M.; Henriksen, U. B.; Ahrenfeldt, J.; Arnavat, M. P. Design, construction and operation of a low-tar biomass (LTB) gasifier for power applications. *Energy* **2020**, *204*, 117944. DOI
36. Liakakou, E. T.; Vreugdenhil, B. J.; Cerone, N.; et al. Gasification of lignin-rich residues for the production of biofuels via syngas fermentation: comparison of gasification technologies. *Fuel* **2019**, *251*, 580-92. DOI
37. Čespiva, J.; Wnukowski, M.; Niedzwiecki, L.; et al. Characterization of tars from a novel, pilot scale, biomass gasifier working under low equivalence ratio regime. *Renew. Energy* **2020**, *159*, 775-85. DOI
38. Marchelli, F.; Cordioli, E.; Patuzzi, F.; et al. Experimental study on H<sub>2</sub>S adsorption on gasification char under different operative conditions. *Biomass. Bioenergy* **2019**, *126*, 106-16. DOI
39. Kilpimaa, S.; Runtti, H.; Kangas, T.; Lassi, U.; Kuokkanen, T. Physical activation of carbon residue from biomass gasification: novel sorbent for the removal of phosphates and nitrates from aqueous solution. *J. Ind. Eng. Chem.* **2015**, *21*, 1354-64. DOI
40. Výtisk, J.; Čespiva, J.; Jadlovec, M.; Kočí, V.; Honus, S.; Ochodek, T. Life cycle assessment applied on alternative production of carbon-based sorbents - a comparative study. *Sustain. Mater. Technol.* **2023**, *35*, e00563. DOI
41. Kumdhithahutsawakul, L.; Jirachaisakdeacha, D.; Kantha, U.; et al. Removal of hydrogen sulfide from swine-waste biogas on a pilot scale using immobilized *Paracoccus versutus* CM1. *Microorganisms* **2022**, *10*, 2148. DOI PubMed PMC
42. Wang, H.; Larson, R. A.; Runge, T. Impacts to hydrogen sulfide concentrations in biogas when poplar wood chips, steam treated wood chips, and biochar are added to manure-based anaerobic digestion systems. *Bioresour. Technol. Rep.* **2019**, *7*, 100232. DOI
43. Silverstein, R. M.; Bassler, G. C. Spectrometric identification of organic compounds. *J. Chem. Educ.* **1962**, *39*, 546. DOI
44. Korus, A.; Ravenni, G.; Loska, K.; Korus, I.; Samson, A.; Szlęk, A. The importance of inherent inorganics and the surface area of wood char for its gasification reactivity and catalytic activity towards toluene conversion. *Renew. Energy* **2021**, *173*, 479-97. DOI
45. Zhou, C.; Chen, Y.; Xing, X.; et al. Pilot-scale pyrolysis and activation of typical biomass chips in an interconnected dual fluidized bed: comparison and analysis of products. *Renew. Energy* **2024**, *225*, 120339. DOI
46. Tan, J.; Li, W.; Tang, L.; Chen, X.; Liu, H.; Wang, F. Study on the pyrolysis characteristics and char gasification kinetics of pre-separated automobile shredder residues. *J. Environ. Chem. Eng.* **2024**, *12*, 112520. DOI
47. Zeghioud, H.; Fryda, L.; Djelal, H.; Assadi, A.; Kane, A. A comprehensive review of biochar in removal of organic pollutants from wastewater: characterization, toxicity, activation/functionalization and influencing treatment factors. *J. Water. Process. Eng.* **2022**, *47*, 102801. DOI
48. Wu, L.; Guan, Y.; Li, C.; et al. Free-radical behaviors of co-pyrolysis of low-rank coal and different solid hydrogen-rich donors: a critical review. *Chem. Eng. J.* **2023**, *474*, 145900. DOI
49. Jiang, X.; Wang, W.; Hu, B.; Zhang, B.; Li, K. Formation mechanism of CH<sub>4</sub> during lignin pyrolysis: a theoretical study. *J. Energy. Inst.* **2022**, *100*, 237-44. DOI
50. Hwang, S. Y.; Lee, G. B.; Kim, H.; Park, J. E. Influence of mixed methods on the surface area and gas products of activated carbon. *Carbon. Lett.* **2020**, *30*, 603-11. DOI
51. Zhou, Q.; Cheung, C. S.; Leung, C. W.; Li, X.; Huang, Z. Explosion characteristics of bio-syngas at various fuel compositions and dilutions in a confined vessel. *Fuel* **2020**, *259*, 116254. DOI
52. Skřínský, J.; Vereš, J.; Čespiva, J.; Ochodek, T.; Borovec, K.; Koloničný, J. Charakterystika explozji gazu syntezowego z procesu zgazowania. *Inżynieria. Mineralna.* **2020**, *2*, 195-200. DOI
53. Shivapuji, A. M.; Dasappa, S. Influence of fuel hydrogen fraction on syngas fueled SI engine: fuel thermo-physical property analysis and in-cylinder experimental investigations. *Int. J. Hydrogen. Energy* **2015**, *40*, 10308-28. DOI
54. Solferini de Carvalho, F.; Rufino, C. H.; Malheiro, O. E.; et al. Experimental investigation of hydrogen-producer gas mixtures in an optically accessible SI engine. *Int. J. Hydrogen. Energy* **2024**, *58*, 500-13. DOI
55. Lin, X.; Lei, H.; Wang, C.; et al. The effects of pore structures and functional groups on the catalytic performance of activated carbon catalysts for the co-pyrolysis of biomass and plastic into aromatics and hydrogen-rich syngas. *Renew. Energy* **2023**, *202*, 855-64. DOI
56. Villardon, A.; Alcazar-Ruiz, A.; Dorado, F.; Sanchez-Silva, L. Enhancing carbon dioxide uptake in biochar derived from husk biomasses: optimizing biomass particle size and steam activation conditions. *J. Environ. Chem. Eng.* **2024**, *12*, 113352. DOI
57. Zango, Z. U.; Garba, A.; Haruna, A.; et al. A systematic review on applications of biochar and activated carbon derived from biomass as adsorbents for sustainable remediation of antibiotics from pharmaceutical wastewater. *J. Water. Process. Eng.* **2024**, *67*, 106186. DOI
58. Bélanger, N.; Gariépy, Y.; Francis, M.; et al. Assessment and enhancement of starch-based biochar as a sustainable filler in styrene-butadiene rubber composites via steam and CO<sub>2</sub> activation treatments. *Biomass. Bioenergy* **2024**, *184*, 107174. DOI
59. Mlonka-Mędrala, A.; Gołombek, K.; Buk, P.; Cieślík, E.; Nowak, W. The influence of KCl on biomass ash melting behaviour and high-temperature corrosion of low-alloy steel. *Energy* **2019**, *188*, 116062. DOI
60. Scala, F. Particle agglomeration during fluidized bed combustion: Mechanisms, early detection and possible countermeasures. *Fuel. Process. Technol.* **2018**, *171*, 31-8. DOI
61. Damø, A. J.; Cafaggi, G.; Pedersen, M. N.; et al. Full-scale investigations of initial deposits formation in a cement plant co-fired with coal and SRF. *Fuel* **2023**, *344*, 128058. DOI
62. Mlonka-Mędrala, A.; Magdziarz, A.; Gajek, M.; Nowińska, K.; Nowak, W. Alkali metals association in biomass and their impact on ash melting behaviour. *Fuel* **2020**, *261*, 116421. DOI
63. Sieradzka, M.; Mlonka-Mędrala, A.; Magdziarz, A. Comprehensive investigation of the CO<sub>2</sub> gasification process of biomass wastes using TG-MS and lab-scale experimental research. *Fuel* **2022**, *330*, 125566. DOI

64. Attalla, M.; Sadek, S.; Salem, A. M.; Shafie, I. M.; Hassan, M. Experimental study of solar powered ice maker using adsorption pair of activated carbon and methanol. *Appl. Therm. Eng.* **2018**, *141*, 877-86. [DOI](#)
65. Taghipour, H.; Amjad, Z.; Aslani, H.; Armanfar, F.; Dehghanzadeh, R. Characterizing and quantifying solid waste of rural communities. *J. Mater. Cycles. Waste. Manag.* **2016**, *18*, 790-7. [DOI](#)
66. Tuck, C. O.; Pérez, E.; Horváth, I. T.; Sheldon, R. A.; Poliakoff, M. Valorization of biomass: deriving more value from waste. *Science* **2012**, *337*, 695-9. [DOI](#) [PubMed](#)